

PAPER • OPEN ACCESS

## The Optimized Welding Spot Structure Parameters of Corrugated Plate Component Based on Variance Analysis

To cite this article: Zhang Xiang *et al* 2019 *IOP Conf. Ser.: Mater. Sci. Eng.* **563** 032041

View the [article online](#) for updates and enhancements.

# The Optimized Welding Spot Structure Parameters of Corrugated Plate Component Based on Variance Analysis

Zhang Xiang, Jia Wang\*, Qingzhong He, Manjiao Chen

Sichuan University of Science & Engineering, Yibin Sichuan 644000, China

\*Corresponding author, e-mail: 86444713@qq.com

**Abstract:** According to the fourth strength theory, this paper adopted equivalent stress to simulate fatigue life. Firstly, ANSYS was used to simulate equivalent stress in single-row welding, and variance analysis was used to analyze and process the simulation results to obtain the effect law of horizontal spacing and diameter of welding spot on the stress. Then, the equivalent stress of corrugated plate component, which was welded in triangular solder joint arrangement, was analyzed and treated with the method of variance analysis, and the effect law was obtained. In terms of the structure parameters of welding spot, the left and right margin of welding spot in the first row is 10 mm, 7 in number, and the center of the welding spot is 3.5 mm away from the upper boundary; the left and right margin of welding spot in the second row is 91.7 mm, 6 in number, and the center of the welding spot is 4.5 mm away from the upper boundary; both rows have a diameter of 5 mm and a horizontal spacing of 163.3 mm. Moreover, the actual fatigue life of physical test is more than  $2.0E7$  times, meeting the requirements of the working condition.

## 1. Introduction

The high-temperature flue gas from the boiler tail is used by air preheater, which is a kind of preheating equipment, to heat the air before entering the boiler to improve the boiler combustion efficiency and reduce the heat loss [1-3]. In the literature [4-9], Yu, L, Naphon, P. et al. expounded the harm of air leakage to its efficient and stable operation and proposed corresponding improvement measures. For most of the current air preservers, there exist some problems such as wear resistance, weak corrosion resistance, and difficult dust cleaning [10-15]. In view of the above defects, a new type of sealing device called corrugated plate spring flexible contact seal is developed, which has the advantages of good sealing performance, good resilience, stiffness and automatic wear compensation, etc. At the present stage, flexible sealing technology is one of the most advanced and the best sealing technologies in the air preheater sealing technology [16-19]. The corrugated plate component studied in this paper is one of the many flexible sealing devices of air preservers. It has been widely used because of its strong sealing adaptive ability, simple structure and low cost. In actual work, the corrugated plate component of air preheater is subjected to a symmetrical cyclic load, and its fatigue performance directly affects the sealing performance. Therefore, it is necessary to study the fatigue performance of corrugated plate component. However, S316L is adopted to form the corrugated plate component by the overall rolling, and S316L has good welding performance. Therefore, spot welding is used to assemble and connect the corrugated plate component.

In the finite element simulation of spot welding parts structure, multiple modeling methods can be used to replace the welding spot. Jiang-Liang, D. et al. [20] studied four models such as ACM2 model, solid model, CWELD model, and RBE2 rigid beam model to replace the welding spot diameter and



summarized the advantages and disadvantages of various models according to the specific case analysis. Cong Li [21] et al. studied the laser welding of biological tissue, established the skin double-layer structure model based on the theory of biological heat transfer, and simulated the effect of the change of laser spot size on the thermal deformation of laser surface welding. Cong-Cheng, L. [22] et al. combined the initial stress and strain field with the continuous damage mechanics theory, the element failure and crack initiation criteria to present the prediction model of crack initiation under creep or fatigue interaction. Moreover, the finite element simulation of crack initiation under the creep-fatigue interaction of the initial defect-free structure was achieved and the factors, which influenced the crack initiation life, were analyzed. Cheng-Zhi, S. [23] et al. used the prediction method of spot welding fatigue life based on equivalent structural stress to simulate the fatigue life of resistance spot welding under the two states of tower joint and stripping. Therefore, it is feasible to study welding fatigue performance and other quality performance of mechanical parts with simulation calculation.

In this paper, simulation accuracy, modeling efficiency, the characteristics of the welding principle and the stressing feature of the welding parts are considered comprehensively. Then the Imprint Faces function of the Design Modeler module in Workbench was used to mark the circular seal surface, which was used to set up the finite element model of welding spot, and combination function (Bonded) of Contact module was used to bond together the corresponding circular seal surface of the adjacent two pieces of seal corrugated plate components. Therefore, the circular spot welding connection problem can be converted to the Contact problem of the seal surface. Firstly, the equivalent stress of the corrugated plate component was analyzed and treated with the method of variance analysis without a repeated test of double factors, and the better horizontal distance of the welding spot was selected. Then, the equivalent stress of corrugated plate component, which was welded in triangular solder joint arrangement, was analyzed and treated with the method of variance analysis without a repeated test of double factors, and the optimal fatigue life was selected according to the results. Finally, the physical test method was used to verify the optimized structure parameters of the welding spot. The research methods and ideas adopted in this paper can provide a reference for other researchers or students who study the role of welding or component connection. In addition, the research results of this paper can also provide a reference for industrial production and welding parts processing.

## 2. Material and Methods

### 2.1 Selection of optimization method for welding structure parameters

The methods, which are used to estimate fatigue life, include nominal stress method and local stress-strain method. Nominal stress method is applicable to high cyclic variable stress conditions with cycle times above  $1.0E4$ . The corrugated plate component needs to be replaced every 3 ~ 5 years, and the speed of air preheater is 1.0 r/min, in which the corrugated plate component works under the cyclic stress of about 200 N, and the expected life is about  $1.0E6$  times. Therefore, the nominal stress method is used to study the fatigue performance of corrugated plate component.

The fatigue life simulation is carried out on the basis of the  $S-N$  curve. The equation is shown in formula (1) [24]. In the formula,  $\sigma$  is stress,  $m$  and  $C$  are material constants determined by experiments, and  $N$  is life. Take the logarithm of both sides of the equation and arrange to get the formula (2).

$$\sigma^m N = C \quad (1)$$

$$m \lg \sigma + \lg N = \lg C \quad (2)$$

When  $N = 1.0E6$ ,  $\sigma_{10^6} = \delta\sigma$ . Based on the type of materials and heat treatment, and combined with the table for estimation of fatigue characteristics of commonly used domestic materials [24], the reasonable value of  $\sigma$  is obtained to determine the  $S-N$  curve of materials.

It is generally believed that the maximum principal stress can be used to explain the fatigue damage mechanism, that is, the degree of damage to the isotropic probability of atomic escape can be

represented. However, this theory is only applicable when one of the three maximum principal stresses dominates [25-27]. Sometimes, however, although unidirectional load of the structure is great, no damage has been caused for the reason that the tests of strength of materials are generally under unidirectional loading strength. However, product structure has its complexity, so there is a big difference between the stress condition of the structural parts and that of the single tensile parts. Therefore, there may not exist the maximum principal stress that can be dominant. At this point, it is more reasonable to use the fourth strength theory (distortion theory) to analyze the yield damage, that is to say, no matter what the material stress state is, the main factor causing material yield failure is the distortion energy density, and the equation is shown in formula (3). In the formula, the main stress ( $\sigma_1, \sigma_2, \sigma_3$ ) is transformed to equivalent stress ( $\sigma_s$ ) [28]. The results of previous studies show that the simulation results of fatigue life have a good correspondence with the equivalent stress.

$$\sigma_s = \{[(\sigma_1 - \sigma_2)^2 + (\sigma_1 - \sigma_3)^2 + (\sigma_2 - \sigma_3)^2] / 2\}^{1/2} \leq [\sigma] \quad (3)$$

On this basis, the specific research process is shown in Figure 1.

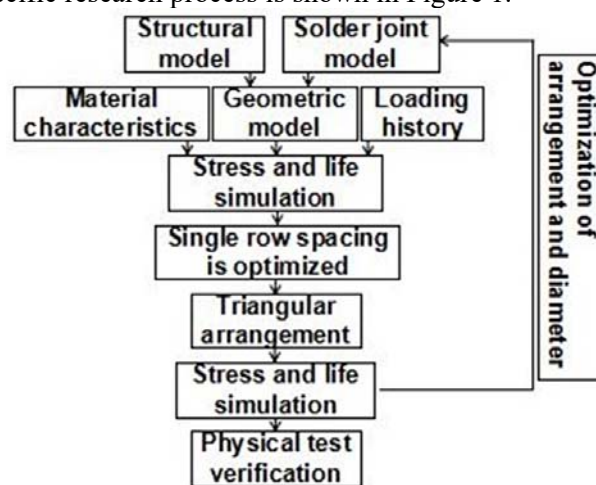


Figure 1. Optimization process of welding spot structure parameters

## 2.2 Welding model and loading method of the corrugated plate component

Corrugated plate component is made of S316L stainless steel completely. The nominal yield limit of the material is greater than or equal to 177 MPa, the tensile strength is greater than or equal to 480 MPa, the elongation is greater than or equal to 45%, the hardness is less than or equal to HV 200, and the elastic modulus is about 200 GPa. In the ANSYS Workbench, the corrugated plate component model is divided into grids. Considered the effect of grid quality and quantity on simulation accuracy and speed, the grid cell size is set to 5 mm, and then the grid around the welding spot model is subdivided and optimized with the cell size of 0.5 mm. The final grid model is shown in Fig. 2. The total number of grids is 651485, and the total number of nodes is 1296158.

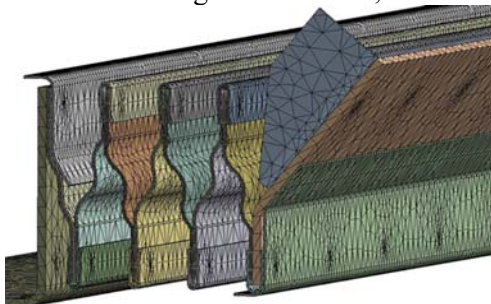


Figure 2. Corrugated plate component grid model and direction of the load

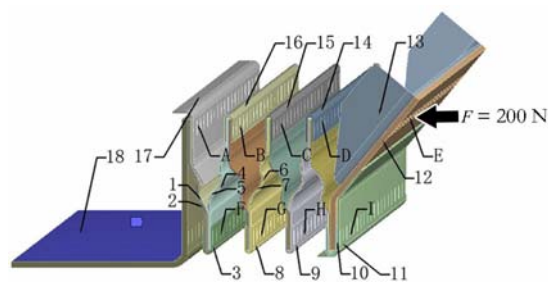


Figure 3. The position of spot weld and direction of the load

The spot-welding joint model and its loading mode are shown in Fig.3, where A ~ I is the welding spot. Parts 1 and 2 are 0.6 mm thick corrugated plate sealing sheets, parts 4 ~ 7 are 0.4 mm thick

corrugated plate sealing sheets, parts 3, 8, 9, 10, 14 ~ 16 are 0.6 mm thick u-type joint plates, parts 11, 13, 17 and 18 are 0.6 mm thick folding plates, and part 12 is 1.2 mm thick groove friction sealing plates. The u-shaped plate is wrapped with four adjacent corrugated plate sealing plates, which are fixedly connected through spot welding. The folding plates and grooved friction sealing plates are then spot-welded on both ends of the corrugated plate components. The end of the folding plate 18 is installed at the corresponding position of the air preheater, and the end of the folding plate 13 is combined with other parts to drive the periodic compression and stretching of corrugated plate component, which plays the role of the circular elastic sliding seal. After determining the S-N curve of the material, the Fatigue strength factor  $K_f$  is set to 0.8, and the stress ratio  $r$  is set to -1 (i.e., symmetric cyclic alternating stress) in the Fatigue Tool module. The surface load is applied to groove friction seal plate 12 along the X (horizontal) direction, and its size is 200 N. At the same time, a fixed constraint is applied to the folding plate 18.

### 3. Results and discussion

First of all, the welding points are arranged in a rectangular area of 1000 mm long and 8 mm wide. In consideration of the welding spot diameter, the integral value between 2 ~ 7 mm is selected for the welding spot diameter, and the maximum number of welding spot rows is 2 ( $R$  is for the number of rows of welding spot,  $N$  is for the number of the first welding spot, and  $D$  is for the diameter of welding spot).

#### 3.1 Single row welding method

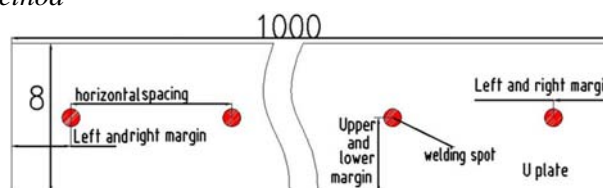


Figure 4. Single row solder joint arrangement

When single-row welding is used, welding spot arrangement is shown in Figure 4 schematic. The welding spot is arranged along the length direction of u-shaped plate and evenly distributed 11 ~ 20 welding spots. The welding spot layout specific parameters are shown in Table 1.

Table 1. Welding spot layout of the corrugated plate component

Solder joints number	Left and right margin/mm	Upper and lower margin/mm	Horizontal spacing/mm
1	10	4	98、89.1、81.7、75.4、70、65.3、61.3、57.6、54.4、51.6

The equivalent stress and fatigue life of the corrugated plate component are shown in Table 2. Under the arrangement of some welding spots, the fatigue life of the corrugated plate component is less than  $1.0E6$  times (see the underlined data in the table). Under the different horizontal spacings and diameters of welding spots, it can be seen from Table 2 that the equivalent stress of the corrugated plate component is all less than 177 MPa, meeting the requirements of static strength of the corrugated plate component. The linear accumulation law of Miner only applies to the linear part of the S-N curve, that is, the part within the elastic limit range of the material [29-34], while the equivalent stress of the corrugated plate component is far less than the nominal yield limit, which satisfies the using conditionals of the linear accumulation law of Miner.

Table 2. Simulation results of the equivalent stress and fatigue life of corrugated plate component during single row welding (stress [MPa], fatigue life [times])

Arrangement mode	Welding spot diameter											
	2 mm		3 mm		4 mm		5 mm		6 mm		7 mm	
	stress	life	stress	life	stress	life	stress	life	stress	life	stress	life

RIN11	66.82	<u>9.05e5</u>	65.4	1.01e6	65.27	1.02e6	65.51	1.01e6	66.38	<u>9.40e5</u>	65.66	1.00e6
RIN12	65.99	<u>9.73e5</u>	66.22	<u>9.54e5</u>	64.65	1.05e6	66.02	<u>9.70e5</u>	65.6	1.00e6	63.67	1.10e6
RIN13	66.95	<u>8.95e5</u>	69.66	<u>7.12e5</u>	61.87	1.20e6	67.73	<u>8.37e5</u>	63.73	1.09e6	67.19	<u>8.77e5</u>
RIN14	66.3	<u>9.47e5</u>	67.81	<u>8.32e5</u>	63.2	1.12e6	64.31	1.07e6	65.89	<u>9.82e5</u>	65.02	1.03e6
RIN15	113.96	<u>7.44e4</u>	82.17	<u>2.75e5</u>	58.9	1.39e6	44.03	3.17e6	44.31	3.14e6	43.77	3.20e6
RIN16	64.27	1.07e6	68.37	<u>7.94e5</u>	65.76	<u>9.92e5</u>	65.06	1.03e6	64.59	1.05e6	65.09	1.03e6
RIN17	64.93	1.03e6	70.13	<u>6.85e5</u>	64.07	1.08e6	64.9	1.04e6	60.16	1.30e6	64.63	1.05e6
RIN18	63.23	1.12e6	70.15	<u>6.85e5</u>	65.36	1.01e6	65.75	<u>9.94e5</u>	65.81	<u>9.88e5</u>	65	1.03e6
RIN19	65.45	1.01e6	68.3	<u>7.98e5</u>	63.63	1.10e6	65.28	1.02e6	60.45	1.28e6	66.95	<u>8.95e5</u>
RIN20	62.68	1.15e6	63.46	1.11e6	64.37	1.06e6	64.54	1.05e6	61.63	1.21e6	66.07	<u>9.66e5</u>

In order to study whether or not the horizontal spacing and diameter of welding spots have a significant impact on the equivalent stress of corrugated plate components, the equivalent stress in Table 2 is analyzed by the variance analysis of the two-factor unreplicated test, and the analysis results are shown in Table 3. For a given significance level of 0.01, the  $F$  distribution table shows that  $F_{0.01}(5, 45) = 3.45$  and  $F_{0.01}(9, 45) = 2.83$ .  $F_A$  is no more than 3.45, indicating that the diameter of the welding spot has no significant effect on the equivalent stress of corrugated plate component.  $F_B$  is no more than 2.83, indicating that the horizontal spacing of welding spots has no significant effect on the equivalent stress of corrugated plate component.

Table 3. Analysis of variance

Differences between the source		$SS$		$df$		$MS = SS/df$		$F = MS/MS_E$
Factor A (diameter)	$SS_A$	598.93	$df_A$	5	$MS_A$	119.79	$F_A$	1.48
Factor B (pitch)	$SS_B$	27.99	$df_B$	9	$MS_B$	3.11	$F_B$	0.04
Error	$SS_E$	3645.4	$df_E$	45	$MS_E$	81.01		
Sum	$SS_T$	4272.3	$df_T$	59				

(note:  $SS_A$ ,  $SS_B$  -- sum of squares of deviation caused by factor A and factor B;  $SS_E$  -- sum of squared error;  $SS_T$  -- sum of total deviation squared;  $df$  -- degrees of freedom for each sum of squares;  $MS_A$ ,  $MS_B$  -- the mean square between the groups of factor A and factor B, and  $MS_E$  -- error mean square;  $F_A$ ,  $F_B$  --  $F$  test of factor A and factor B)

For welding parts, the contour parameters at the actual welding joint are random along the weld length direction, and the resulting stress concentration will also change randomly [25-27, 35]. Microscopically, the isotropy of escape of atoms or molecules at the stress concentration is destroyed, which leads to the increase of the probability of an atom or molecule that escapes in some directions. Thus, the transient void created by the escape of atoms or molecules cannot be completely filled by atoms or molecules that have escaped elsewhere. Furthermore, it greatly promotes the formation and accumulation of fatigue damage. In actual welding, when the stress concentration area near the welding spot is superimposed on each other, the local stress of corrugated plate component will be uneven, and the slight deformation of the contour at the welding spot will make the stress distribution fluctuate. The simulation results are consistent with the actual situation.

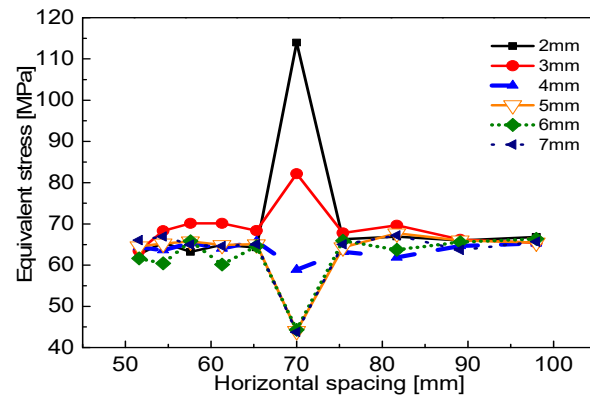


Figure 5. The equivalent stress at different horizontal spacings and diameters of the welding

In order to observe the effect of welding spot horizontal spacing and diameter on the equivalent stress of corrugated plate component more intuitively, the data in Table 2 is plotted into broken lines, as shown in Fig. 5. On the whole, the equivalent stress of corrugated plate component does not change significantly with the change of welding spot horizontal spacing or diameter, which may be caused by the number of welding spots. The connection effect of welding spot diameter on corrugated plate component and the micro-defects of corrugated plate component increase with the increase of welding spot diameter, leading to the increase of the randomness of stress distribution. Locally, when the welding spot horizontal spacing is 70 mm, the equivalent stress of corrugated plate component fluctuates greatly with the change of welding spot diameter, and its minimum value is also the minimum value in the entire picture. Therefore, the better horizontal spacing of the welding spot is 70 mm.

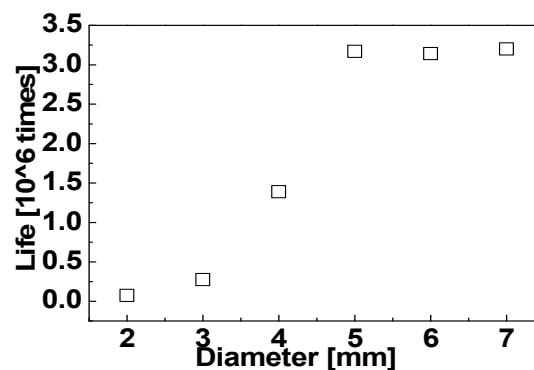


Figure 6. Effect of welding spot diameter on fatigue life

When the welding spot horizontal spacing is 70 mm, the effect of the welding spot diameter changing on the equivalent stress of corrugated plate component is shown in Fig. 6. When the diameter of the welding spot varies between 2 ~ 5 mm, the equivalent stress of corrugated plate component increases with the increase of the diameter of the solder joint. This may be the joint effect of the welding spot on the corrugated plate component, which magnifies with the increase of the diameter of the welding spot. When the diameter of the welding spot varies between 5 ~ 7 mm, the equivalent stress of corrugated plate component does not increase obviously with the increase of the diameter of the solder joint, and it is only slightly fluctuating. It may be that the microscopic defects of corrugated plate component increase with the increase of the solder spot diameter, resulting in the deterioration of the mechanical properties of corrugated plate component due to the microscopic defects, which is equal to or even more than the effect of the strengthened connection due to the increase of solder spot diameter. In order to further optimize the structure parameters of the solder joint, the arrangement mode of the solder joint is adjusted and optimized.



### 3.2 Triangulation of solder joint

When two rows of welding are used, the center of the first-row welding spots is 3.5 mm away from the upper boundary, the left and right edge distance of the welding spots is 10 mm, and the welding spot is uniformly distributed. The center of the second-row welding spots is 4.5 mm away from the upper boundary, and the welding spots are located on the center line of any two adjacent welding points in the first row. Thus, the solder joints of the second row are one less than that of the first row and any adjacent three solder joints form an isosceles triangle. Horizontal spacing refers to the distance between two adjacent solder joints in the horizontal direction. At this point, please refer to Fig.7 for the specific arrangement of welding spots.

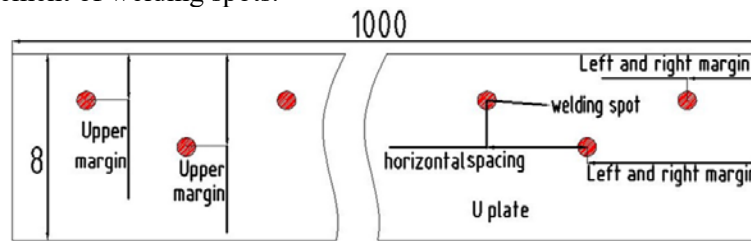


Figure 7. Welding spot triangular arrangement

In the above solder joint arrangement mode, through the setting of the corresponding solution, the simulation results of equivalent stress and fatigue life of the corrugated plate component are shown in Table 4. Under some solder joint arrangement modes, the fatigue life of the corrugated plate component is less than  $1.0 \times 10^6$  (see the underlined data in the table).

Table 4. Simulation results of equivalent stress and fatigue life of corrugated plate component when the welding spot is arranged in a triangular shape (stress [MPa], fatigue life [times])

Arrangement mode	Welding spot diameter											
	2 mm		3 mm		4 mm		5 mm		6 mm		7 mm	
	stress	life	stress	life	stress	life	stress	life	stress	life	stress	life
R1N15	114.0	<u>7.44e4</u>	82.17	<u>2.75e5</u>	58.9	1.39e6	44.03	3.17e6	44.31	3.14e6	43.77	3.20e6
R2N15	66.34	<u>9.44e5</u>	64.54	1.05e6	66.34	<u>9.44e5</u>	66.79	<u>9.08e5</u>	67.8	<u>8.32e5</u>	71.51	<u>6.13e5</u>
R2N10	98.3	<u>1.28e5</u>	72.43	<u>5.70e5</u>	61.87	1.20e6	63.86	1.09e6	63.41	1.11e6	66.26	<u>9.51e5</u>
R2N9	67.3	<u>8.69e5</u>	64.02	1.08e6	64.34	1.06e6	64.04	1.08e6	65.4	1.01e6	67.36	<u>8.64e5</u>
R2N8	66.2	<u>9.55e5</u>	65.88	<u>9.82e5</u>	65.73	<u>9.95e5</u>	61.86	1.20e6	67.3	<u>8.69e5</u>	68.04	<u>8.16e5</u>
R2N7	56.58	1.57e6	62.91	1.14e6	56.3	1.59e6	55.65	1.64e6	58.46	1.42e6	63.19	1.12e6
R2N6	56.6	1.56e6	61.91	1.19e6	56.24	1.59e6	57.94	1.46e6	59.5	1.34e6	56.06	1.61e6

In order to study whether or not the welding spot diameter and horizontal spacing have a significant impact on the stress status of corrugated plate component, the equivalent stress of corrugated plate component in the triangular arrangement mode in Table 4 is analyzed by variance without a repeated test of double factors. The results are shown in Table 5. For a given significance level of 0.01, the  $F$  distribution table shows that  $F_{0.01}(5, 25) = 3.85$ .  $F_C$  is less than or equal to 3.85, which indicates that under the condition of constant horizontal distance between welding points, the variation of welding spot diameter has no significant effect on equivalent stress when the horizontal distance of the welding spot stay the same.  $F_D$  is greater than or equal to 3.85, indicating that the variation of the horizontal distance of the welding spot has a significant effect on the equivalent stress when the diameter of the welding spot stay the same. Compared the analysis result of Table 3 with that of Table 5, the triangular arrangement mode of welding spot can obviously change the stress state of corrugated plate component.

Table 5. Analysis of variance

Differences between the source	SS	df	MS = SS/df	F = MS/MS <sub>E</sub>
Factor C(diameter)	SS <sub>C</sub>	5	MS <sub>C</sub>	F <sub>C</sub>
Factor D (pitch)	SS <sub>D</sub>	5	MS <sub>D</sub>	F <sub>D</sub>



Error	$SS_E$	906.45	$df_E$	25	$MS_E$	36.26
Sum	$SS_T$	1865.17	$df_T$	35		

(note:  $SS_C$ ,  $SS_D$  -- sum of squares of deviation caused by factor C and factor D;  $SSE$  - sum of squared error;  $SS_T$  - sum of total deviation squared;  $df$  - degrees of freedom for each sum of squares;  $MS_C$ ,  $MS_D$  -- the mean square between the groups of factor C and factor D, and  $MS_E$  -- error mean square;  $F_C$ ,  $F_D$  --  $F$  test of factor C and factor D)

Fig. 8 shows the impact of welding spot diameter on the fatigue life of the corrugated plate component under each arrangement mode. It can be seen from Fig. 8 that the fatigue life changes significantly with the variation of welding spot diameter in the R1N15 arrangement mode, which is consistent with the conclusion drawn in Fig. 5, that is, the variation of welding spot diameter has a significant impact on the stress of corrugated plate component when the welding spot is single-row and the horizontal spacing is 70 mm. While in the triangular arrangement, the fatigue life does not change significantly with the variation of welding spot diameter, and there are only slight fluctuations. It is consistent with the result of variance analysis in Table 5, that is, the change of welding spot diameter has no significant effect on the equivalent stress. The fluctuation may be caused by the increase of microscopic defects of materials with the increase of the welding spot diameter and the random superposition of damage in the area affected by stress concentration.

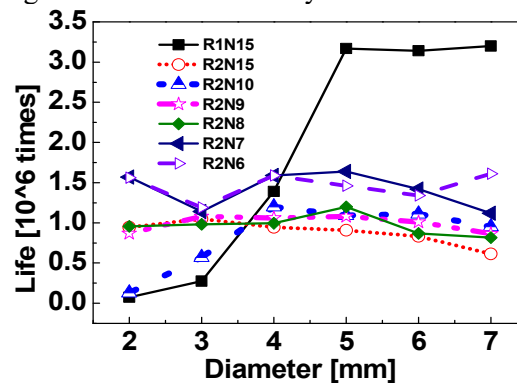


Figure 8. Effect of welding spot diameter on fatigue life

Fig. 9 shows the effect of horizontal spacing on the fatigue life of the corrugated plate component in the triangular arrangement of welding spots. Locally, the fatigue life varies slightly with the variation of the horizontal spacing of the welding spots. As a whole, the fatigue life increases with the increase of the horizontal distance between the solder joints. In the triangular arrangement mode, when the horizontal spacing changes in a small range, the stress concentration area of the corrugated plate component is randomly superimposed, resulting in small fluctuations. However, when the horizontal spacing changes significantly, the stress changes greatly, and the joint effect of welding spot on the corrugated plate component and the random superposition effect on the stress concentration area around the welding spot intersects with each other, resulting in a great change in the fatigue life. It is consistent with the results of variance analysis in Table 5, in which the variation of the horizontal distance between the solder joints has a significant effect on the equivalent stress, while the diameter of the solder joints stay the same.

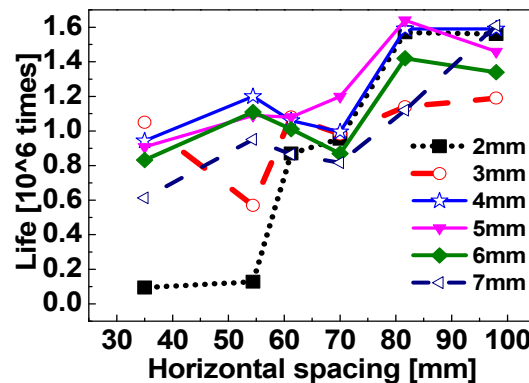


Figure 9. Effect of the horizontal spacing of solder joints on fatigue life

In order to study the effect of triangular arrangement and single-row welding on the stress and fatigue life of corrugated plate component further, 11, 13, 15, 17 and 19 solder joints are selected to be welded in single-row respectively according to the arrangement of triangles listed in Table 4 and the analysis results, and the effect on the fatigue life is analyzed. Comparing the above analysis results and that of the solder joint triangle arrangement, considering the different effects of different arrangement under different number of solder joints on the corrugated plate component, the above five kinds numbers of solder joint can be divided into two groups, which takes the number 13 as the boundary, and line charts are drawn respectively, as shown in Figure 10 and Figure 11.

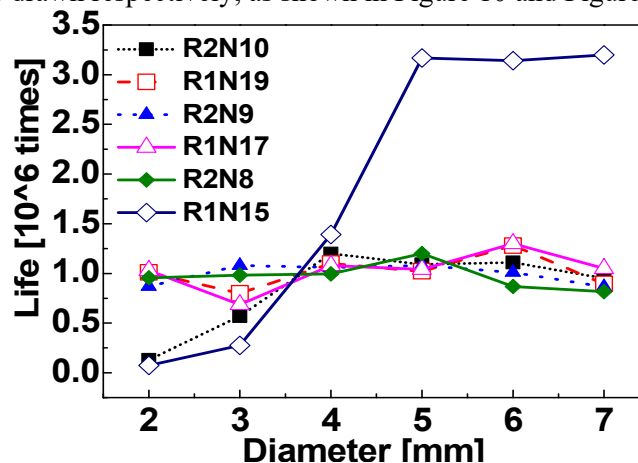


Figure 10. Line chart with no obvious advantage

It can be seen from Figure 10 that in the case of the same number of solder joints, there is no such arrangement mode as triangular arrangement mode and single-row welding mode, which will lead to the better fatigue life of corrugated plate component as the diameter of solder joints changes. This situation may be the result of the effect of different arrangements on the stress of corrugated plate components, the effect of the increase of welding spot diameter on the connection of corrugated plate component, and the effect of the increase of microscopic defects on the fatigue performance of corrugated plate component due to the increase of welding spot diameter.

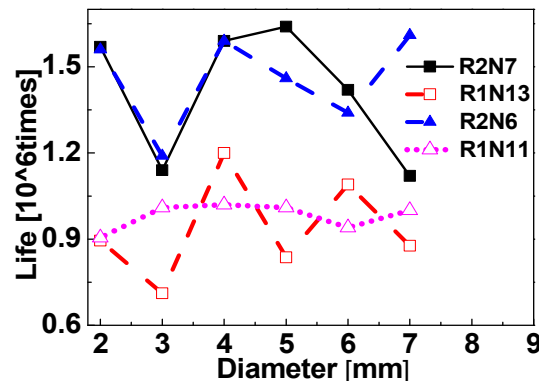


Figure 11. Broken line diagram in which a triangle arrangement is dominant

It can be seen from Figure 11 that under the same number of solder joints, the fatigue life of corrugated plate component is better than that of the corresponding single-row welding spot no matter how the welding spot diameter changes. This situation may occur because the arrangement mode shown in Figure 11 shows that the triangular arrangement mode has a significant improvement in the stress condition of the corrugated plate component. Therefore, its fatigue life is better than that of single-row welding.

According to Table 4, under the arrangement mode of R2N7D5, the fatigue life of corrugated plate component is the largest in the triangular arrangement mode, and this arrangement mode is also in the dominant range of triangular arrangement mode. At this point, the equivalent stress simulation result of corrugated plate component is 55.65MPa, and the fatigue life simulation result is 1.64E6 times. The simulation cloud diagram of fatigue life is shown in Figure 12.

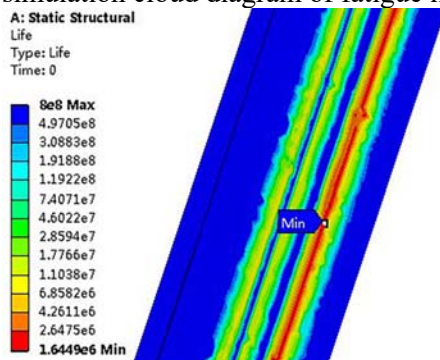


Figure 12. Cloud diagram of fatigue life of corrugated plate component

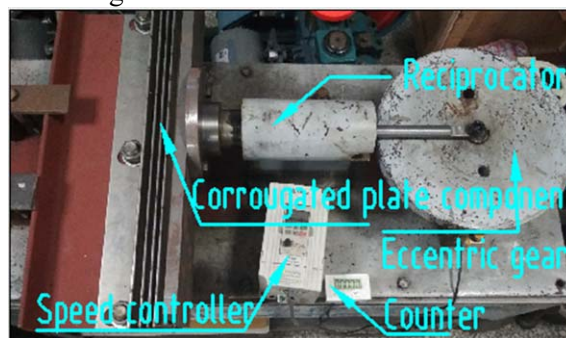


Figure 13. Fatigue test bench of the corrugated plate component

#### 4. Experimental verification

Three corrugated plate components are processed according to R2N7D5 arrangement. In the reciprocating motion test bench of the connecting rod shown in Fig. 14, physical tests are carried out under the case of exceeding the operating load. The eccentric wheel drives the reciprocating motion mechanism with the rotating speed of 20 revolutions per second, which brings about the cyclic compression deformation with a minimum of 8 mm and a maximum of 15 mm. According to the test, the minimum fatigue life of the sample is about 2.04E7 times. It can be seen that the actual fatigue life of the corrugated plate component of the air pre-heater meets the design requirements.

#### 5. Conclusion

(1) On the whole, the horizontal spacing and diameter of the welding spot have no significant effect on the stress of corrugated plate component when the welding spots are welded in single-row. However, when the horizontal distance between the solder joints is 70 mm, the variation of solder joint diameter has a significant impact on the stress of the corrugated plate component.

(2) In the triangular arrangement mode, the horizontal spacing of the welding spot stay the same, and the change of welding spot diameter has no significant effect on the stress of the corrugated plate component. When the diameter of the solder joint stay the same, the horizontal spacing of the solder joint has a significant effect on the stress of the corrugated plate component.

(3) After comprehensive consideration, it is considered that the better arrangement of the welding spot is a triangle arrangement. In the arrangement, the left and right edge distance of the first welding spot is 10 mm, 7 in number, and the center of the welding spot is 3.5 mm away from the upper boundary; the left and right edge distance of the second welding spot is 91.7 mm, 6 in number, and the center distance of the welding spot is 4.5 mm away from the upper boundary. The diameter of the two rows of welding spot is both 5 mm and its horizontal spacing is 163.3 mm. At this point, the fatigue life simulation result of corrugated plate component is  $1.64E6$  times. In the physical test, the actual fatigue life exceeds  $2.0E7$  times, meeting the requirements of fatigue performance of corrugated plate component in the actual working condition.

### Acknowledgements

The Authors wish to thank Zi gong municipal science and technology bureau for support of Development of elastic sealing device with a corrugated plate for air presser(NO.2016JZ04) and Sichuan University of Science & Engineering for support of Development of fatigue performance test experimental device for an elastic sealing component of air preserver(NO.Y2017025). The first author would like to express appreciation to associate professor Professor Wang Jia, Professor He Qingzhong and Lecturer Chen Manjiao for valuable discussions that improved the quality and presentation of the paper. At the same time, the first author also thanks Professor Zhang Ronghui from the intelligent transportation system research center of the school of engineering, Sun Yat-sen University for giving valuable suggestions to this paper and giving the first author corresponding help in the paper writing.

### References

- [1] Chen, L. X., Xie, M. N., Zhao, P. P., Wang, F. X., Hu, P., & Wang, D. X. (2018). A novel isobaric adiabatic compressed air energy storage (IA-CAES) system on the base of volatile fluid. *Applied Energy*, 198-210.
- [2] Speerforck, A., Ling, J., Aute, V., Radermacher, R., & Schmitz, G. (2017). Modeling and simulation of a desiccant assisted solar and geothermal air conditioning system. *Energy*, 2321-2336.
- [3] Feng-Liang, H. Study on heat transfer and resistance characteristics of corrugated plate with disturbing hole in rotary air preconditioner. Hangzhou: Zhejiang University, 2015.
- [4] Yu, L. Hua-Zhong, L., Xiao-Gang, C., et al. Air leakage treatment of rotary air preheater and examples. *boiler manufacturing*, 2002(4):27-29.
- [5] Naphon, P. (2010). On the performance of air conditioner with heat pipe for cooling air in the condenser. *Energy Conversion and Management*, 51(11), 2362-2366.
- [6] Warsinger, D. M., Servi, A., Van Belleghem, S., Gonzalez, J. V., Swaminathan, J., Kharraz, J., ... & Lienhard, J. H. (2016). Combining air recharging and membrane superhydrophobicity for fouling prevention in membrane distillation. *Journal of Membrane Science*, 241-252.
- [7] Attia, H., Osman, M. S., Johnson, D., Wright, C. J., & Hilal, N. (2017). Modelling of air gap membrane distillation and its application in heavy metals removal. *Desalination*, 27-36.
- [8] Li, Q., Zheng, C., Shirazi, A., Mousa, O. M., Moscia, F., Scott, J., & Taylor, R. A. (2017). Design and analysis of a medium-temperature, concentrated solar thermal collector for air-conditioning applications. *Applied Energy*, 1159-1173.
- [9] Wang, H., Cai, W., & Wang, Y. (2017). Optimization of a hybrid ejector air conditioning system with PSOGA. *Applied Thermal Engineering*, 1474-1486.
- [10] Jia-Yang, H. Estimation and analysis of dust accumulation in rectangular flue of air presser to dust collector. *Hongshui river*, 2017, 36(2):58-60.

- [11] Elminshawy, N. A., Siddiqui, F. R., Farooq, Q. U., & Addas, M. F. (2017). Experimental investigation on the performance of earth-air pipe heat exchanger for different soil compaction levels. *Applied Thermal Engineering*, 1319-1327.
- [12] Thalfeldt, M., Kurnitski, J., & Latosov, E. (2018). Exhaust air heat pump connection schemes and balanced heat recovery ventilation effect on district heat energy use and return temperature. *Applied Thermal Engineering*, 402-414.
- [13] Cordeau, S., & Barrington, S. (2010). Heat balance for two commercial broiler barns with solar preheated ventilation air. *Biosystems Engineering*, 107(3), 232-241.
- [14] Yan, H., Deng, S., & Chan, M. (2016). Operating characteristics of a three-evaporator air conditioning (TEAC) system. *Applied Thermal Engineering*, 883-891.
- [15] Chandrasekar, M., Senthilkumar, T., Kumaragurubaran, B., & Fernandes, J. P. (2018). Experimental investigation on a solar dryer integrated with condenser unit of split air conditioner (A/C) for enhancing drying rate. *Renewable Energy*, 375-381.
- [16] Hu, L., Wei-Ping, Z., Lei-Yuan, Z., et al. Calculation and analysis of friction power of flexible seal of rotary air preheater. *Chinese journal of electrical engineering*, 2013, 33(14):93-100.
- [17] Darvishi, H., Azadbakht, M., & Noralahi, B. (2018). Experimental performance of mushroom fluidized-bed drying: Effect of osmotic pretreatment and air recirculation. *Renewable Energy*, 201-208.
- [18] Pabst, C., Feckler, G., Schmitz, S., Smirnova, O., Capuano, R., Hirth, P., & Fend, T. (2017). Experimental performance of an advanced metal volumetric air receiver for Solar Towers. *Renewable Energy*, 91-98.
- [19] Chel, A., Janssens, A., & De Paepe, M. (2015). Thermal performance of a nearly zero energy passive house integrated with the air–air heat exchanger and the earth–water heat exchanger. *Energy and Buildings*, 53-63.
- [20] Jiang-Liang, D. Chang-De, W. Xiao-Ping, X. et al. Finite element modeling method research and case application of spot welding connection. *Modern manufacturing engineering*, 2014(9):74-80.
- [21] Li, C., Wang, K., & Huang, J. (2018). Simulation of the effect of spot size on temperature field and weld forming in laser tissue welding. *Optik*, 315-323.
- [22] Cong-Cheng, L. Hong-Yang, J. Lian-Yong, X., et al. Finite element simulation of crack initiation under creep fatigue interaction. *Journal of welding*, 2016, 37(8):5-8.
- [23] Cheng-Zhi, S. and Guang-Jun, C. Prediction of fatigue life of resistance spot welding based on equivalent structure stress. *Journal of welding*, 2011, 32(1):105-108.
- [24] Shao-Bian, Z. *Anti-fatigue design -- methods and design*. Beijing: mechanical industry press, 1997.
- [25] Pugno, N., Ciavarella, M., Cornetti, P., & Carpinteri, A. (2006). A generalized Paris' law for fatigue crack growth. *Journal of the Mechanics and Physics of Solids*, 54(7), 1333-1349.
- [26] Mcevily, A. J., Eifler, D., & Macherauch, E. (1991). An analysis of the growth of short fatigue cracks. *Engineering Fracture Mechanics*, 40(3), 571-584.
- [27] Ziha, K. (2016). Relating fracture mechanics and fatigue lifetime prediction. *Materials Science and Engineering A-structural Materials Properties Microstructure and Processing*, 167-176.
- [28] Jie-Min Liu, Ya-Zhen Sun, Xu-Zhong Yuan, et al. *Material mechanics course*. China electric power press, 2015.
- [29] Miner M A. Cumulative damage in fatigue. *Journal of Applied Mechanics*, 1945, 12(3): A159-164.
- [30] Ciavarella, M., Antuono, P. D., & Demelio, G. (2017). A simple finding on variable amplitude (Gassner) fatigue SN curves obtained using Miner's rule for unnotched or notched specimen. *Engineering Fracture Mechanics*, 178-185.
- [31] Butlewski, M., Dahlke, G., Drzewiecka, M., & Pacholski, L. (2015). Fatigue of Miners as a Key Factor in the Work Safety System. *Procedia Manufacturing*, 4732-4739.

- [32] Jardin, A., Leblond, J., Berghezan, D., & Portigliatti, M. (2010). Definition and experimental validation of a new model for the fatigue of elastomers incorporating deviations from Miners linear law of cumulative damage. *Procedia Engineering*, 2(1), 1643-1652.
- [33] Sun, Q., Dui, H., & Fan, X. (2014). A statistically consistent fatigue damage model based on Miner's rule. *International Journal of Fatigue*, 16-21.
- [34] Mezyk, A., Klein, W., Fice, M., Pawlak, M., & Basiura, K. (2016). Mechatronic model of continuous miner cutting drum driveline. *Mechatronics*, 12-20.
- [35] Yan-Hua, Z. *Fatigue analysis of welding structures*. Beijing: chemical industry press, 2013.